Subattosecond keV beats of the high-harmonic x-ray field produced with few-cycle mid-IR laser pulses: Magnetic-field effects

A. S. Emelina,[1] M. Yu. Emelin,[1,*] and M. Yu. Ryabikin[1,2]
[1]*Institute of Applied Physics, Russian Academy of Sciences, Nizhny Novgorod 603950, Russia*
[2]*Lobachevsky State University of Nizhny Novgorod, Nizhny Novgorod 603950, Russia*
(Received 31 July 2015; published 1 April 2016)

Using the theoretical description beyond the dipole approximation, we examine the impact of the electron magnetic drift caused by a strong midinfrared laser field on the feasibility and ultimate limitations of the method proposed recently [C. Hernández-García *et al.*, Phys. Rev. Lett. **111**, 033002 (2013)] as a route to the generation of zeptosecond x-ray waveforms; this method relies on the interference of high-harmonic emission from multiple reencounters of the electron wave packet with the ion. We show that the electron magnetic drift serves as the spectral filter changing the relative weights of the contributions to the high-harmonic signal from different rescattering events. For a range of driving wavelengths in the midinfrared, the use of the control of the carrier-envelope phase, occasionally in combination with the spectral filtering, to cope with the magnetic drift effect is shown to facilitate the production of intense high-contrast keV beats of durations shorter than 0.8 attosecond. The limitations on the laser wavelengths usable for implementing this approach are determined by the growing unamendable imbalance between the contributions of interfering paths and by an overall decline in the efficiency of high-harmonic generation at longer driving wavelengths.

DOI: 10.1103/PhysRevA.93.043802

I. INTRODUCTION

The advent of high-power midinfrared femtosecond laser sources has opened up new perspectives in the research of strong-field laser-matter interactions [1–3]. One of the most impressive benefits of using mid-IR sources to drive the processes associated with the recollisions of electrons with the parent ions in laser-induced ionization [4,5] is a dramatic extension of the plateau in the high-harmonic spectrum produced in gases to much higher photon energies [6–8].

High-order harmonic generation (HHG) in gases is a three-step process, in which, according to the semiclassical model [5], the electron is optical field ionized, accelerated by the oscillating electric field, and driven back to the parent ion to emit a high-energy photon. The spectrum of HHG driven by visible or near-infrared laser fields is plateaulike, with the cutoff energy determined by the sum of the atomic ionization potential I_p plus the electron's kinetic energy $3.17U_p$ at the recollision instant, where $U_p = e^2E_0^2/4m\omega_0^2$ is the average energy of electron oscillations in an ac electric field of amplitude E_0 and frequency ω_0 (ponderomotive energy). The extension of the plateau produced with longer-wavelength driving lasers is due to the proportionality of the ponderomotive energy to the square of the laser wavelength.

The use of mid-IR driving laser pulses has been demonstrated experimentally to produce high-harmonic x-ray emission spanning keV bandwidth [8] that, in the Fourier limit, is capable of supporting few-attosecond pulses. However, it is extremely challenging to achieve this limit because of the need to compensate across this enormous bandwidth the attosecond chirp [9] inherent to the HHG process. An alternative and relatively simple route for breaking the attosecond barrier has been proposed recently [10]. This proposal relies on the theoretical observation that the spectral structure of the HHG x-ray emission driven by ultrashort mid-IR pulses, in contrast to that observed at near-infrared driving wavelengths, exhibits pronounced peaks that have been identified as originating from the electrons liberated during different half cycles of the laser field that then reencounter the parent ion multiple times. The interference of contributions from different reencounters can form a regular pattern of interference beats whose duration can reach the zeptosecond time scale for driving wavelengths approaching 10 μm if the carrier-envelope phase (CEP) of the laser pulse is adjusted properly.

One of the potential obstacles to producing zeptosecond waveforms using this scheme is the magnetic field of the laser pulse, whose influence is expected to significantly modify HHG from neutral atoms if driving wavelengths of about 10 μm or longer are used [11]. The influence of the magnetic part of the Lorentz force on the motion of a classical electron driven by a subrelativistically strong electromagnetic field is known to be manifested in drifting the electron trajectories in the laser pulse propagation direction [12]. If this drift is comparable to the width of the electron wave packet at the recollision instant, reduced efficiency of HHG is expected [13–15]. Moreover, since the magnetic drift accumulated by an electron moving along a particular trajectory depends on the path length, as well as on the field it experiences during this motion, the contributions of different trajectories to the HHG signal are affected by the magnetic field differently; this results in reshaping the HHG spectrum [11,16]. At visible or near-infrared laser wavelengths, these magnetic-field effects can only be non-negligible for multicharged ions [16] that can withstand the subrelativistic intensities without substantial ionization, whereas more weakly bound atomic systems get ionized at intensities far below the relativistic regime. In contrast to that, at a driving wavelength of 10.6 μm both the yield and spectral shape of high-order harmonics produced in neutral atoms have been shown to be strongly modified by the magnetic-field effects at any intensity sufficient for ionization [11]. It is therefore important to examine the

*emelin@ufp.appl.sci-nnov.ru

limitations imposed by the magnetic-field effects on the practicability of the above-mentioned scheme for zeptosecond x-ray waveform generation for this driving wavelength range.

Note that, in the context discussed here, the effect of the magnetic drift in HHG driven by long-wavelength lasers was analyzed briefly in [10]. From simple arguments based on the comparison of the magnetic drift with the width of the electron wave packet, it was concluded that the use of laser wavelengths longer than 9 μm to produce ultrashort x-ray waveforms is unpromising since, according to the estimations made, the magnetic-drift-induced drop in efficiency of HHG at a relevant laser intensity is an order of magnitude already at this driver wavelength. Due to the latter fact, the duration of efficiently produced x-ray beats is estimated to be limited to the level of 1 as.

It should be noted that the approach that led to these conclusions was overly simplistic. The magnetic drifting was considered in [10] as a uniform motion at the average velocity calculated for the case of a sinusoidal laser field. This approximation can be successfully used in the case of a multicycle laser pulse [17], but strictly speaking, it is not applicable in the case of a few-cycle pulse. Note furthermore that the keV beats discussed here appear at the trailing part of the laser pulse [10] rather than near its maximum. In this case, the cycle-averaged drifting velocity is not constant, but rather decreases with time. It is therefore expected that the limitations found in [10] can be relaxed. Finally, since the above-mentioned keV beats result from the interference of high-harmonic emission from electron subpackets launched at different instants during an ultrashort laser pulse, an adequate description of the path-specific electron magnetic drift is critical to find correctly the outcome of this interference.

The present paper provides a detailed analysis of the above issues based on the theoretical description beyond the dipole approximation.

II. THEORETICAL METHOD

In this work, we use the single-active-electron approximation [18,19] to describe the interaction of an atom with a strong electromagnetic field. In this case, the full-dimensionality (three-dimensional) treatment of the atomic nonlinear response to a laser field in the subrelativistic regime can be done by a direct numerical integration of the time-dependent Schrödinger equation in the framework of the nonrelativistic nondipole approximation (see, e.g., [20,21]). However, the required computational efforts increase dramatically with increasing wavelength, making the three-dimensional (3D) numerical calculations prohibitively time-consuming for a range of wavelengths of interest to the present study. For this reason, the theoretical study in this paper is based on an analytical approach. We use the quantum-mechanical treatment of HHG within the strong-field approximation [22] modified properly to take into account the atomic bound-state depletion and the effect of the magnetic field of a laser pulse on the dynamics of the released electron [11,23].

In the following, we assume that the laser pulse propagates in the positive z direction and is linearly polarized along the x axis. To account for the influence of the magnetic field of the laser pulse, one should take into consideration the full spatial dependence of the vector potential $\mathbf{A}(t-z/c)$. Given the smallness of the localization scale of the ionized electron wave packet in comparison with the laser wavelength, the decomposition of the vector potential in a series over the propagation coordinate can be used; as a rule, it suffices to retain only the linear term giving the first-order correction in $1/c$ beyond the dipole approximation $\mathbf{A}(t)$ [13,15,24]. We note also that for the ionization processes in the long-wavelength regime, the spin of the electron can be safely ignored [25].

Our study has shown that in the conditions addressed here, the depletion of the medium is negligible; hence, the equation for the laser-induced dipole moment of the atom can be represented in the following simplified form, which differs from Lewenstein's original formula [22] in that it takes into account, in the lowest order in $1/c$, the magnetic-field effects (hereinafter, atomic units are used):

$$x(t) = i\int_0^t d\tau \left(\frac{\pi}{\varepsilon + i\tau/2}\right)^{3/2} d_x^*[\mathbf{p}_{st}(t,\tau) - \mathbf{A}(t)] \times d_x[\mathbf{p}_{st}(t,\tau) - \mathbf{A}(t-\tau)]E(t-\tau) \times \exp[-iS(\mathbf{p},t,\tau) - iS_m(\mathbf{p},t,\tau)] + \text{c.c.}, \quad (1)$$

where t is the current time; τ is the time of the electron's free motion in the laser field after release into the continuum; $E(t)$ is the electric field of the laser pulse; ε is the regularization parameter, which can be chosen to be small; $\mathbf{p}$ is the electron's canonical momentum, whose stationary components are written as

$$p_{st,x}(t,\tau) = \frac{1}{\tau}\int_{t-\tau}^{t} \frac{A(t')}{c} dt', \quad (2)$$

$$p_{st,z}(t,\tau) = \frac{p_{st,x}^2}{c} - \frac{1}{2c\tau}\int_{t-\tau}^{t} \frac{A^2(t')}{c^2} dt' \quad (3)$$

(c is the speed of light);

$$S(\mathbf{p},t,\tau) = \int_{t-\tau}^{t} \left[\frac{1}{2}\left(p_x - \frac{A(t')}{c}\right)^2 + I_p\right] dt' \quad (4)$$

is the quasiclassical action describing, in the dipole approximation, the free motion of the electron in the laser field;

$$S_m(\mathbf{p},t,\tau) = \int_{t-\tau}^{t} \frac{1}{2}\left[p_z - \frac{p_x A(t')}{c^2} + \frac{A^2(t')}{2c^3}\right]^2 dt' \quad (5)$$

is the nondipole correction to the quasiclassical action related to the electron's magnetic drift; I_p is the atomic ionization potential; and $d_x(\mathbf{p})$ is the x component of the dipole matrix element corresponding to the transition between the ground state and the continuum, which, in the plane-wave approximation valid for highly energetic continuum states, can be written as

$$d_x(\mathbf{p}) = i\frac{2^{7/2}(2I_p)^{5/4}}{\pi}\frac{p_x}{(\mathbf{p}^2 + 2I_p)^3}. \quad (6)$$

Equations (1)–(6) allow one to perform the calculations beyond the dipole approximation, whereas the transition to the dipole approximation can be done by setting $p_{st,z}$ and S_m equal to zero.

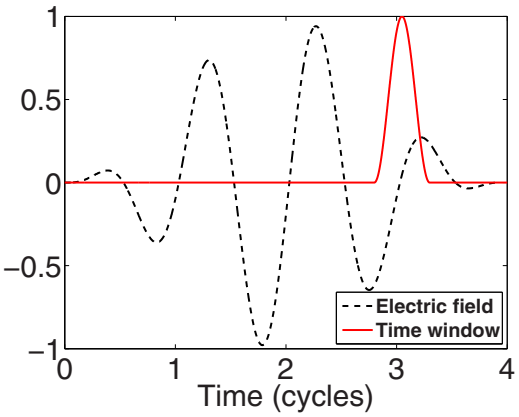

FIG. 1. Normalized electric field $E(t)/E_0$ of the laser pulse [see (7), $\varphi = \pi/8$] and the time-window function used in the analysis of the HHG signal.

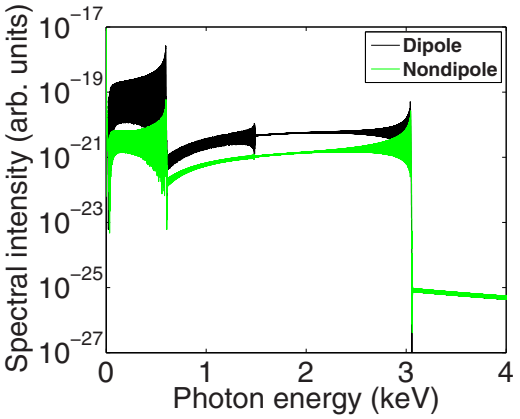

FIG. 2. Spectrum of the selected x-ray burst generated on the trailing part of the laser pulse with $\lambda_0 = 9$ μm and $\varphi = \pi/8$; the results obtained in the dipole approximation and beyond it are shown.

III. RESULTS

The calculations were made for a helium atom driven by a few-cycle laser pulse whose electric field is given by

$$E(t) = E_0 \sin^2\left(\frac{\pi ct}{4\lambda_0}\right)\sin\left(\frac{2\pi ct}{\lambda_0} - \varphi\right) \tag{7}$$

[see Fig. 1 for the normalized field $E(t)/E_0$ with $\varphi = \pi/8$, black dashed line]. The peak intensity of the laser pulse was chosen to be equal to $3.4 \times 10^{14}\mathrm{W/cm_2}$, whereas the central wavelength λ_0 was varied between 9 and 16 μm; different values of the carrier-envelope phase φ were considered. With the few-cycle driving field used here, the generated x-ray field is dominated by two femtosecond bursts originating from the electrons liberated around the two strongest crests of the laser field. The second burst, which is produced at the trailing part of the laser pulse, turns out to exhibit super-high-frequency oscillations arising from the interference of high-harmonic emission from two different reencounters of the electron wave packet with the parent ion [10]. Specifically, the first of the two interfering trajectories contributing to this femtosecond burst belongs to the set of shortest electron trajectories (lasting less than one optical cycle, $\tau < T$) between ionization and recombination events, whereas the second interfering trajectory corresponds to longer electron excursion ($T < \tau < 1.5T$) after ionization near the earlier of the two strongest field crests. To concentrate on the analysis of the interference of these contributions, we used temporal filtering with the sine-squared window function (see red solid line in Fig. 1) centered at the above-mentioned second burst in the HHG signal; the width of this time window was equal to the laser half cycle.

Figure 2 shows the spectral content of the x-ray burst generated on the trailing part of the laser pulse (7) with $\lambda_0 = 9$ μm and $\varphi = \pi/8$. The black line represents the spectrum calculated in the dipole approximation. This spectrum exhibits two pronounced peaks at photon energies near 0.6 and 3.05 keV. The positions of these peaks correspond to the cutoffs of the plateaus in the spectra of harmonics emitted due to the second and first reencounters of the electron wave packet with the ion, respectively (see [10]). The height and width of each plateau are determined, respectively, by the weight of the related trajectory and the electron energy at the recollision instant.

The two-peak structure of the spectrum, such as that shown in Fig. 2, leads to the modulation of the femtosecond x-ray burst into a waveform of ultrashort beats. Obviously, the beating contrast of the resulting waveform is highest when the two spectral peaks are of comparable weights. In Fig. 2, the relative weight between the lower- and higher-energy peaks in the spectrum calculated for the dipole case is substantially different. However, by attenuating the first peak using the spectral filter (the transmission through the Al filter can be used in this particular case [10]) the two peaks can be equalized. As a result, a perfectly contrasted waveform can be obtained with the width of each beat being about 1 as [see Fig. 3(a)], in agreement with [10].

The spectrum of the same x-ray burst calculated beyond the dipole approximation is represented by the green line in Fig. 2. Importantly, it turns out that the effect of the magnetic field, which is typically detrimental to HHG, does not lead to fatal consequences in the case under consideration. Indeed, the emission spectrum in this case still exhibits two distinct peaks. Moreover, the magnetic field of the laser pulse serves here as a spectral filter, which in certain cases may favorably alter the relative weights of the peaks in the HHG spectrum. Just such a case can be seen in Fig. 2. In the nondipole spectrum, the low-energy peak is significantly reduced, whereas its high-energy counterpart is only slightly attenuated. This difference can be explained by the fact that the drift due to the magnetic part of the Lorentz force is greater for those electrons that take a longer excursion between ionization and recombination. Furthermore, as far as the electron trajectories of interest relate to the trailing part of the laser pulse, the trajectory launched at the earlier time is driven by a stronger field and hence exhibits larger magnetic drift. That is why the contribution from the double-reencounter trajectory to the HHG emission (low-energy peak) is affected much more by the magnetic field compared to that from the single-reencounter trajectory (high-energy peak). In the case shown in Fig. 2, only a small additional spectral filtering is required to equalize the two

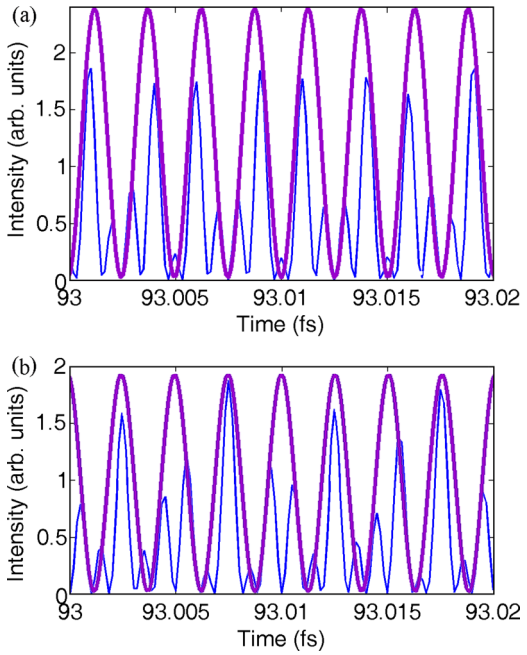

FIG. 3. Temporal structure of the x-ray burst generated on the trailing part of the laser pulse with $\lambda_0 = 9$ μm and $\varphi = \pi/8$. (a) The dipole and (b) nondipole results. The thick line represents the envelope of the bursts.

peaks. The resulting signal shown in Fig. 3(b) is only about 20% weaker than in the dipole case.

Next, we examine what happens to the HHG spectra at laser wavelengths longer than 9 μm. Figure 4 shows the results of calculations for different wavelengths; all other parameters of the pulse remain fixed. All spectra calculated in the dipole approximation turn out to have the same shape, while the energy gap ΔE between the two dominant peaks increases gradually with the wavelength. This leads to the prediction that, for instance, the characteristic time scale of the beats (which is inversely proportional to ΔE) in a properly filtered HHG signal is about 0.4, like for the case of a 14-μm driving laser. In contrast, the spectral shape of the HHG signal changes dramatically with the driving wavelength if the magnetic-field effects are taken into account. In general, with an increase in the laser wavelength, the magnetic field of the pulse has an increasingly deleterious effect on HHG. Furthermore, due to the above-mentioned significant difference in the magnetic drift between the trajectories responsible for the low- and high-energy peaks, the intensity of the former drops much more sharply with the laser wavelength compared with the latter. Specifically, as the driving wavelength changes from 10.6 to 12 μm, the relative weight between the second and first reencounter contributions drops from 10^{-1} to 10^{-3}; finally, the low-energy peak disappears completely at $\lambda_0 = 14$ μm [see Fig. 4(c)]. As can be deduced from Fig. 4, the minimum duration of the beats attainable in this way is about 0.6 as; however, producing high-contrast zeptosecond modulations can only be achieved by filtering out a significant portion of high-energy emission, hence at the cost of a substantial loss of efficiency.

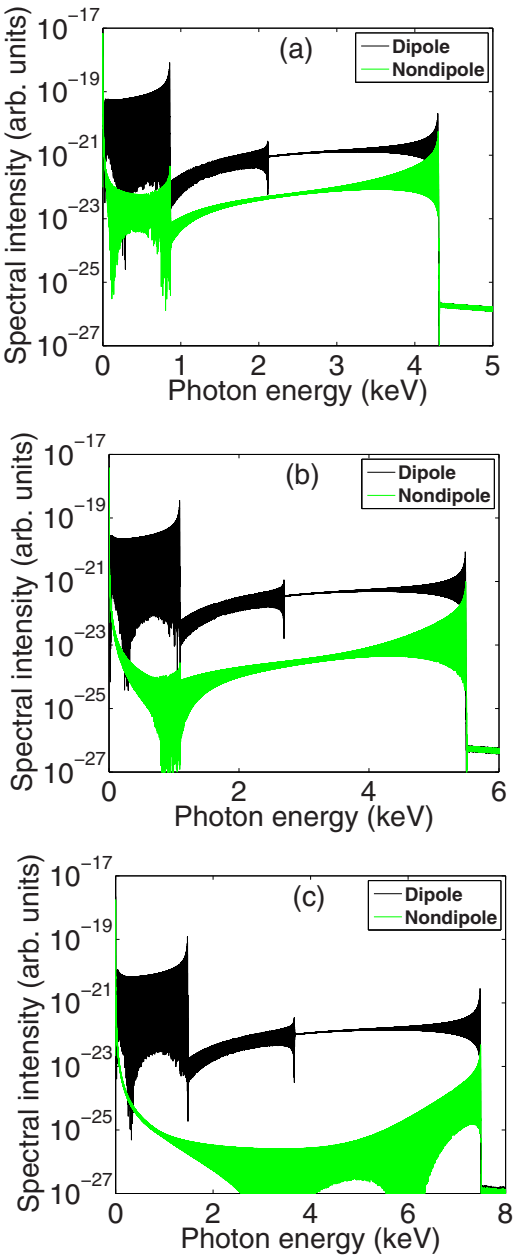

FIG. 4. Spectra of the x-ray burst generated on the trailing part of the laser pulse with $\varphi = \pi/8$ calculated for different wavelengths λ_0: (a) $\lambda_0 = 10.6\,\mu$m, (b) $\lambda_0 = 12$ μm, and (c) $\lambda_0 = 14$ μm. Each plot shows the results obtained in the dipole approximation and beyond it.

In search of ways to more efficiently generate zeptosecond waveforms we further considered the use of the carrier-envelope phase as a control knob. For each wavelength, the optimal CEP value φ_{nd} was found (see Fig. 5), which perfectly balances the relative weight between the first and second reencounter contributions to the HHG spectrum calculated beyond the dipole approximation. In these calculations, the window for temporal filtering was shifted together with the carrier wave; the peak intensity and duration of the laser pulse remained fixed.

It follows from these calculations that when driving wavelengths longer than 9 μm are used, the full-contrast

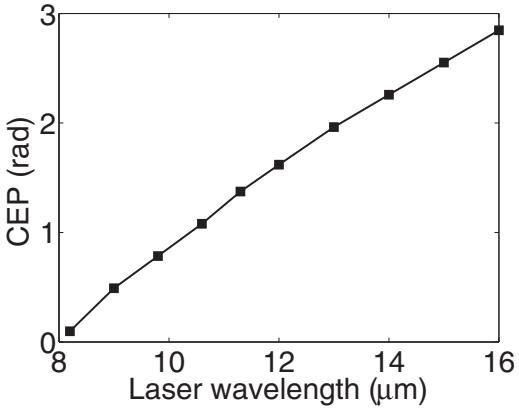

FIG. 5. Wavelength dependence of the optimal carrier-envelope phase balancing the relative weight between the first and second reencounter contributions to HHG in the nondipole case.

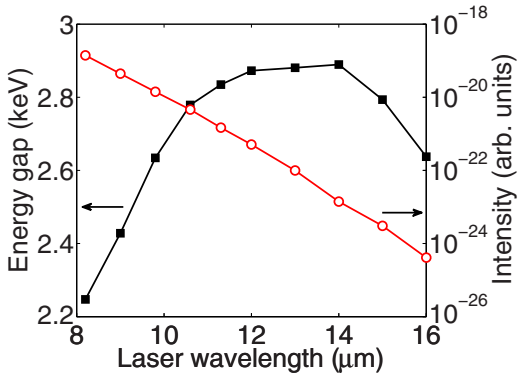

FIG. 7. Energy gap between the low- and high-energy peaks (black squares) and their intensity (red open circles) as functions of the laser wavelength for the x-ray burst generated on the trailing part of the laser pulse with CEP optimized as shown in Fig. 5.

subattosecond beats are produced with significantly higher efficiency if the CEP is adjusted to the φ_{nd} value dictated by the influence of the magnetic field instead of being fixed at the $\varphi_d = \pi/8$ value given by the dipole approximation. A typical example is shown in Fig. 6(a), where, for $\lambda_0 = 10.6\,\mu$m, the intensities of the low- and high-energy peaks are plotted versus the CEP. It is seen that if the CEP is set to

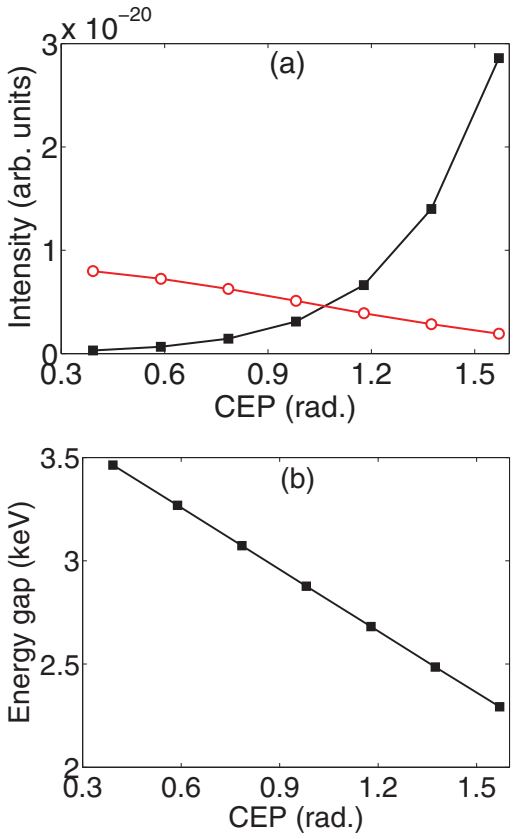

FIG. 6. (a) Intensities of the low-energy (black squares) and high-energy (red open circles) peaks and (b) energy gap between them as functions of the CEP for the x-ray burst generated using a 10.6-μm laser.

$\varphi_{nd} \approx 1.07$, the relative weight between the first and second reencounter contributions is perfectly balanced without the spectral filtering, in contrast to the case of $\varphi_d = \pi/8 \approx 0.39$ shown in Fig. 4, for which the spectral filtering is required to equalize the peaks. The other side of the coin is that, as the CEP is changed from φ_d towards the larger φ_{nd} value, the energy gap between the peaks in the HHG spectrum gets narrower [see Fig. 6(b)]. This can be explained by the fact that when the CEP is adjusted in this way, the position of the femtosecond x-ray burst is shifted along the trailing edge of the laser pulse towards the lower intensity, resulting in lower-energy recollisions. As a consequence, the energy gap ΔE does not increase steadily with the laser wavelength as in Fig. 4, but rather takes its maximum value (about 2.9 keV) at wavelengths in the range of 12–14 μm (see Fig. 7, black squares). At longer driving wavelengths, the growing imbalance between the contributions of interfering paths cannot be compensated without substantial loss of recollision energy. Note also an inevitable decline in HHG yield with increasing wavelength (red open circles in Fig. 7) due to both the magnetic drift of the single-reencounter trajectory, which is relatively small but still nonzero, and the efficiency loss associated with the electron wave-packet spreading [26]. Given all this, a wavelength of 12 μm or slightly shorter appears to be optimal.

From the calculations above, it can be concluded that, in the context discussed here, the CEP control is a double-edged weapon. On the one hand, its use allows enhancing the amplitude and contrast of the generated x-ray waveforms; on the other hand, it may prevent us from producing the shortest possible temporal modulations of the HHG signal. As can be deduced from Fig. 7, the interference beats of about 0.8 as in duration are attainable if the CEP is set to φ_{nd}. Even shorter, although somewhat less intense, beats can be obtained if a CEP in the range of $\varphi_d < \varphi < \varphi_{nd}$ is used in combination with a partial spectral filtering of the single-reencounter contribution.

The complete description of the HHG process needs to analyze the macroscopic propagation in the nonlinear medium. For laser wavelengths of about 10 μm, computing HHG propagation, especially in a 3D geometry, is extremely demanding. In computationally more feasible simulations with a laser wavelength of 1.6 μm, it was shown [27] that,

when a tightly focused laser beam is used, the second return contributes significantly to the macroscopic HHG yield only when the gas jet is near the laser focus, but it barely survives in a setup with a gas jet placed farther behind the focus, which is usually referred to as a better phase-matching condition. In this regard, the following points are, however, worth paying attention to. First of all, the computation in [27] was carried out for a long (30-cycle) laser pulse. In this case, the total HHG yield is determined for the most part by the phase matching at the center of the laser pulse. In contrast, as highlighted above, the quantum-path interference phenomenon addressed here can appear only if a few-cycle laser pulse is used. In this case, the time-dependent phase-matching effects are expected to be important. For example, recent numerical study [28] has shown that harmonics from the long path can be better phase matched at the falling edge than at the leading edge or near the center of the driving pulse. Furthermore, returning to the issue of subattosecond interference patterns, we note that, even if the second reencounter contribution to HHG is not so well phase matched, this can be compensated for by the higher ionization rate present when the corresponding double-return electron trajectory is launched. Finally, it is known that, when tight focusing is used, strong variation of the laser intensity in the interaction region leads to the fact that, normally, phase matching prefers the shorter path contribution because of the smaller field-induced phase accumulated by an electron that follows this path [29]. This factor is, however, less important for HHG driven by either wave-guided or loosely focused laser beams. In the context of the atto and zepto modulations addressed here, the optimal phase-matching conditions for these HHG geometries were discussed in [10]. In particular, by numerical simulation in the plane-wave approximation relevant to these geometries, it was demonstrated that the modulations in the attosecond regime are preserved when considering propagation, at least for the relatively short wavelength of 2 μm considered in the simulation. More rigorous study of the above issue is a highly desirable yet challenging goal.

IV. CONCLUSION

We have presented a detailed study of the influence of the magnetic part of the Lorentz force on the properties of high-harmonic x-ray emission produced in gases driven by few-cycle mid-IR laser pulses. We concentrated on the role of the magnetic-field effects in the modification of the spectral shape of the high-harmonic field and the efficiency of its production in order to investigate the feasibility of the generation of zeptosecond waveforms using the interference of x-ray emissions from multiple recollision events. It has been shown that, in a range of driving wavelengths in the mid-IR, the electron magnetic drift does not destroy completely the mechanism of the formation of subattosecond keV beats, but rather alters the relative weights between different reencounter contributions to the HHG spectrum. The misbalance that emerges between these contributions can be compensated for to some extent using the control of the laser carrier-envelope phase, in some cases in combination with the spectral filtering of the HHG signal. Eventually, intense high-contrast keV beats of durations shorter than 0.8 as are shown to be attainable using few-cycle mid-IR laser pulses with a central wavelength of about 12 μm. The keV waveforms with even shorter durations and higher intensities could be achieved if proper schemes to correct the magnetic drift are found.

ACKNOWLEDGMENTS

We acknowledge financial support from RFBR (Grants No. 14-02-00762 and No. 16-02-00527), the Russian Academy of Sciences (Program No. IV.2.5), and the Presidential Council on Grants of the Russian Federation (Grant No. MK-5935.2015.2).

[1] P. Colosimo, G. Doumy, C. I. Blaga, J. Wheeler, C. Hauri, F. Catoire, J. Tate, R. Chirla, A. M. March, G. G. Paulus, H. G. Muller, P. Agostini, and L. F. DiMauro, Nat. Phys. **4**, 386 (2008).
[2] C. I. Blaga, J. Xu, A. D. DiChiara, E. Sistrunk, K. Zhang, P. Agostini, T. A. Miller, L. F. DiMauro, and C. D. Lin, Nature (London) **483**, 194 (2012).
[3] C. Vozzi, M. Negro, and S. Stagira, J. Mod. Opt. **59**, 1283 (2012).
[4] K. J. Schafer, B. Yang, L. F. DiMauro, and K. C. Kulander, Phys. Rev. Lett. **70**, 1599 (1993).
[5] P. B. Corkum, Phys. Rev. Lett. **71**, 1994 (1993).
[6] B. Shan and Z. Chang, Phys. Rev. A **65**, 011804(R) (2001).
[7] E. J. Takahashi, T. Kanai, K. L. Ishikawa, Y. Nabekawa, and K. Midorikawa, Phys. Rev. Lett. **101**, 253901 (2008).
[8] T. Popmintchev, M.-C. Chen, D. Popmintchev, P. Arpin, S. Brown, S. Ališauskas, G. Andriukaitis, T. Balčiūnas, O. D. Mücke, A. Pugžlys, A. Baltuška, B. Shim, S. E. Schrauth, A. Gaeta, C. Hernández-García, L. Plaja, A. Becker, A. Jaron-Becker, M. M. Murnane, and H. C. Kapteyn, Science **336**, 1287 (2012).
[9] Y. Mairesse, A. de Bohan, L. J. Frasinski, H. Merdji, L. C. Dinu, P. Monchicourt, P. Breger, M. Kovačev, R. Taïeb, B. Carré, H. G. Muller, P. Agostini, and P. Salières, Science **302**, 1540 (2003).
[10] C. Hernández-García, J. A. Pérez-Hernández, T. Popmintchev, M. M. Murnane, H. C. Kapteyn, A. Jaron-Becker, A. Becker, and L. Plaja, Phys. Rev. Lett. **111**, 033002 (2013).
[11] A. S. Emelina, M. Y. Emelin, and M. Y. Ryabikin, Quantum Electron. **44**, 470 (2014).
[12] T. Katsouleas and W. B. Mori, Phys. Rev. Lett. **70**, 1561 (1993).
[13] A. V. Kim, M. Y. Ryabikin, and A. M. Sergeev, Phys. Usp. **42**, 54 (1999).
[14] V. D. Taranukhin, Laser Phys. **10**, 330 (2000).
[15] M. W. Walser, C. H. Keitel, A. Scrinzi, and T. Brabec, Phys. Rev. Lett. **85**, 5082 (2000).
[16] C. C. Chirilă, N. J. Kylstra, R. M. Potvliege, and C. J. Joachain, Phys. Rev. A **66**, 063411 (2002).
[17] S. Palaniyappan, I. Ghebregziabher, A. DiChiara, J. MacDonald, and B. C. Walker, Phys. Rev. A **74**, 033403 (2006).

[18] J. L. Krause, K. J. Schafer, and K. C. Kulander, Phys. Rev. Lett. **68**, 3535 (1992).
[19] J. L. Krause, K. J. Schafer, and K. C. Kulander, Phys. Rev. A **45**, 4998 (1992).
[20] J. R. Vázquez de Aldana and L. Roso, J. Phys. B **35**, 1633 (2002).
[21] M. Y. Emelin, M. Y. Ryabikin, and A. M. Sergeev, J. Exp. Theor. Phys. **106**, 203 (2008).
[22] M. Lewenstein, P. Balcou, M. Y. Ivanov, A. L'Huillier, and P. B. Corkum, Phys. Rev. A **49**, 2117 (1994).
[23] A. S. Emelina, M. Y. Emelin, and M. Y. Ryabikin, J. Opt. Soc. Am. B **32**, 2478 (2015).
[24] N. J. Kylstra, R. M. Potvliege, and C. J. Joachain, J. Phys. B **34**, L55 (2001).
[25] J. R. Vázquez de Aldana and L. Roso, J. Phys. B **33**, 3701 (2000).
[26] J. Tate, T. Auguste, H. G. Muller, P. Salières, P. Agostini, and L. F. DiMauro, Phys. Rev. Lett. **98**, 013901 (2007).
[27] A.-T. Le, H. Wei, C. Jin, V. N. Tuoc, T. Morishita, and C. D. Lin, Phys. Rev. Lett. **113**, 033001 (2014).
[28] F. Wang, L. He, C. Zhai, W. Shi, Q. Zhang, P. Lan, and P. Lu, Phys. Rev. A **92**, 063839 (2015).
[29] P. Salières, A. L'Huillier, and M. Lewenstein, Phys. Rev. Lett. **74**, 3776 (1995).